Research in Astronomy and Astrophysics, 22:055014 (7pp), 2022 May https://doi.org/10.1088/1674-4527/ac5ee9

Testing the Empirical Relationship between Forbush Decreases and Cosmic Ray Diurnal Anisotropy

Jibrin Adejoh Alhassan[1], Ogbonnaya Okike[2], and Augustine Ejikeme Chukwude[1]
[1] Department of Physics and Astronomy, University of Nigeria, Nsukka 400001, Nigeria; jibrin.alhassan@unn.edu.ng
[2] Department of Industrial Physics, Ebonyi State University, Abakaliki 840001, Nigeria
Received 2021 December 25; revised 2022 March 2; accepted 2022 March 14; published 2022 April 29

Abstract

The abrupt aperiodic modulation of cosmic ray (CR) flux intensity, often referred to as Forbush decrease (FD), plays a significant role in our understanding of the Sun–Earth electrodynamics. Accurate and precise determinations of FD magnitude and timing are among the intractable problems in FD-based analysis. FD identification is complicated by CR diurnal anisotropy. CR anisotropy can increase or reduce the number and amplitude of FDs. It is therefore important to remove its contributions from CR raw data before FD identification. Recently, an attempt was made, using a combination of the Fourier transform technique and FD-location machine, to address this. Thus, two FD catalogs and amplitude diurnal variation (ADV) were calculated from filtered (FD1 and ADV) and raw (FD2) CR data. In the current work, we test the empirical relationship between FD1, FD2, ADV and solar-geophysical characteristics. Our analysis shows that two types of magnetic fields - interplanetary and geomagnetic (Dst) - govern the evolution of CR flux intensity reductions.

Key words: methods: data analysis – methods: statistical – catalogs – Sun: coronal mass ejections (CMEs) – (Sun:) solar wind – (Sun:) solar-terrestrial relations – (ISM:) cosmic rays

1. Introduction

Galactic cosmic ray (GCR) intensity flux which is believed to be modulated by solar wind interplanetary magnetic field (IMF) structure, among several other agents, includes periodic and aperiodic components. The periodic category includes cosmic ray (CR) diurnal anisotropy (Okike 2021), 27 days, and 11 yr long term modulations (Oh et al. 2008). CR diurnal anisotropy may be viewed as a periodic, short-term variation in CR flux. It is the portion of the total CR intensity variation with 24 hr periodicity resulting from the Earth's rotation about its axis coupled with the changes of asymptotic cone of acceptance of neutron monitors (NMs, Lockwood 1971). One of the abrupt time-intensity changes of CR flux is a Forbush decrease (FD) event which is named after the pioneer observer of the phenomenon, Forbush (1938). FD is a non-periodic sudden reduction in CR intensity flux caused by interplanetary disturbances (IPDs) in the form of magnetic field enhancements in interplanetary space and high velocity solar wind (Forbush 1938; Barouch & Burlaga 1975; Rao 1976). There are two main kinds of IPDs - sporadic and recurrent. Sporadic IPDs are caused by coronal mass ejections (CMEs) and their interplanetary version-interplanetary coronal mass ejections (ICMEs) while recurrent IPDs are associated with heliospheric current sheets and high-speed plasma flows from coronal holes (CHs) which co-rotate with the Sun (Belov et al. 2001, 2014; Alhassan et al. 2021). FDs from CHs are known to have small magnitudes while those caused by CMEs have large magnitude signatures (Lockwood 1971; Belov et al. 2009; Melkumyan et al. 2019).

Large FDs from isolated NMs appear to be relatively easier to detect than small events. This is attributed to the elusive nature of weak events believed to be caused by the masking tendencies of CR diurnal anisotropies (Barouch & Burlaga 1975). Apart from the challenges associated with weak event detection, Okike (2020a) observed that the inherent CR effects that range from enhanced diurnal anisotropies, signal superposition, periodicities, cycles to short-term random variations on the amplitude and timing of FDs (Cane et al. 1996; Cane & Richardson 2003; Oh et al. 2008; Richardson & Cane 2011) are scarcely removed from raw CR data. This is because the well-known manual method of FD detection is not capable of handling the superposed effects of the "unwanted signals" on CR data (Okike et al. 2021). If the contributions of CR diurnal anisotropies are not considered before FD identification, some of the events selected might just be enhanced diurnal CR anisotropy, pre-increases or pre-decreases that happen before the actual CR depression (Okike & Umahi 2019). Fully automated FD identification that clearly deals with these daunting issues has become the interest of recent works (e.g., Okike & Umahi 2019; Okike 2020a, 2021).

In the study of empirical implication of conducting Chree analysis with data from isolated NM stations, Okike & Umahi (2019) developed an FD-location program which is based on Fourier transformation. Raw CR data are first transformed into

sinusoidal waves. The imaginary part that handles the daily and diurnal variations is discarded. The real part serves as the input signal to the FD-location program. The FD-location program involves several different calculations. Some subroutines detect both small and large transient intensity reductions (minima/pits) as well as increases (maxima/peaks) in CR data. Other sub-modules calculate event magnitude, timing and cataloging of the events identified. The subroutines that track increases in CR flux in the form of solar energetic particles (SEPs) and ground level enhancements (GLEs) are disabled while only reductions in CR flux are selected. While Fourier transformation can remove the slow-moving signal in any data, a step beyond Fourier decomposition that can calculate the FD event date and magnitude is demonstrated in the referred publication.

A direct application of Fourier transform techniques to handle the enhanced diurnal CR wave trains that accompany FDs is a subject of research interest. Okike (2020a) carried out a detailed study of simultaneous and non-simultaneous FDs with focus on the implications of CR diurnal oscillations on FDs at different geographical locations on Earth. This publication developed an FD location algorithm that was used to select FDs from both raw (unprocessed) and Fourier transformed CR data. The code which relies on static mean accepts raw CR data as input signal and is able to calculate both the event time and amplitude concurrently. In addition to the R program, the paper employed Fast Fourier transformation (FFT) in order to decompose the signals into their respective frequency domains to account for the CR diurnal anisotropy that occurs at the time of FDs. For the first time, the algorithm selected two FD catalogs-FD1 (FD from preliminary processed data) and FD2 (FD from unprocessed data). The result of their analysis shows that the amplitude of a CR diurnal wave is about 13 or 20 times the magnitude predicted by Axford (1965) and McCracken & Rau (1965) respectively, but consistent with the high amplitude (≈10%) from Belov (2008).

With some technical improvements in the FD location algorithm, Okike (2021) adjusted for the influence of anisotropy in CR data as well as removal of the solar cycle variations from the observed amplitude of FDs at Climax (CLMX) NM station. This algorithm allows for accurate calibration and ranking of FDs. A comparison of the amplitude of CR diurnal anisotropy with the raw CR data, the Fourier transformed signal and the associated FDs for the year 2003 at CLMX station was demonstrated (see Figure 1). The low velocity and high velocity signals were separated from the raw CR data using the FFT technique. The empirical connection between CR diurnal oscillation and FDs detected from unprocessed (FD2) and Fourier transformed (FD1) CR data is determined utilizing CR data from CLMX NM station for the period 1953–2006. Okike (2021) found strong and statistically significant correlations between FD1, FD2 and amplitude diurnal variation (ADV). The correlation coefficient between FD1 and ADV tends to be higher than that of FD2 and ADV.

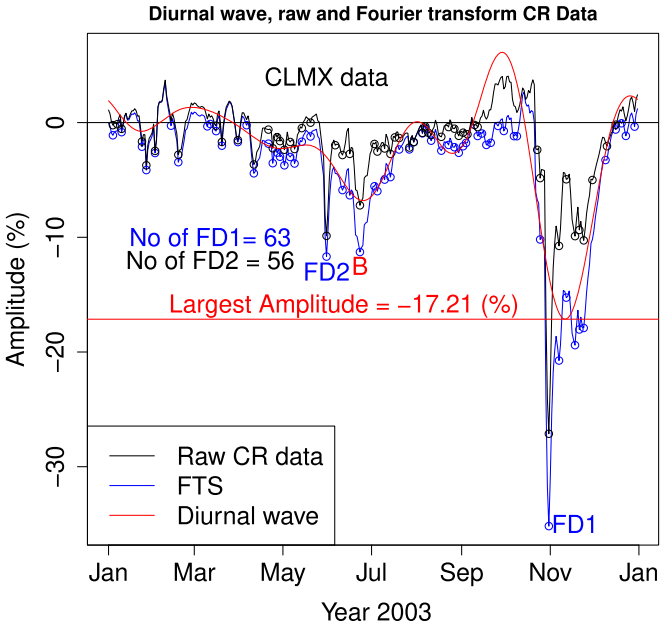

Figure 1. Comparison of the amplitude of CR diurnal anisotropy with the raw CR data, the Fourier transformed signal and the associated FDs for the year 2003 at CLMX station (adapted from Okike 2021).

This underscores the proposition that CR anisotropy is an integral part of CR depressions.

Using numerical filtering techniques on CR data from two isolated NM stations, Apatity (APTY) and Mt. Washington (MTWS), during high solar activity in 1972, Okike & Alhassan (2021), hereafter, Paper I, demonstrated that the low frequency component of CR flux in which CR anisotropy is coded could be disentangled from the rapidly varying portion that contains the FDs. The high velocity signal component is then passed on to an FD location software for accurate event timing and amplitude calculation (FD1) while the magnitudes of the CR diurnal anisotropies (ADV) are obtained from the low-energy spectrum of the raw CR data. An FD location algorithm was further used to estimate the amplitude of FDs from unprocessed CR data (FD2). Thus, two FD catalogs and ADV were calculated from Fourier decomposed (FD1 and ADV) and raw (FD2) CR data. A correlation coefficient of ≈0.98 was found between FDs at APTY and MTWS for both the raw and the transformed data. The high correlation between the FD amplitudes at the two stations may be an indication of the efficiency of the algorithms deployed in Paper I. Presently, there is no FD selection approach that can adequately solve all the problems associated with FD detection, hence the need to validate any selected FD list (Okike 2020b). Obtaining valid FDs is crucial since this approach as been suggested to be an important tool used to examine the electrodynamics of the solar-terrestrial connection (see Paper I).

Table 1
APTY$_{FD1}$, ADV1 and Solar Wind Data

Order	Date	IMF	SWS	Dst	FD1(%)	ADV1(%)
1	1972-01-02	5.70	438	−11	−0.78	0.18
2	1972-01-30	4.30	490	−20	−1.13	−1.69
3	1972-02-15	4.40	560	−17	−3.81	−1.83
4	1972-02-20	7.00	447	−28	−4.98	−1.27
5	1972-02-25	4.40	458	−46	−0.88	−0.46
6	1972-03-07	16.00	596	−36	−2.48	1.63
7	1972-03-10	8.60	388	−16	−3.36	2.12
8	1972-03-15	3.90	336	5	−2.55	2.75
9	1972-03-17	8.50	480	−27	−0.71	2.92
10	1972-03-30	6.70	445	−40	−0.96	3.03
11	1972-04-07	4.20	443	−15	−2.50	2.67
12	1972-04-12	6.00	373	−10	−1.62	2.54
13	1972-04-23	6.50	373	−17	−3.62	2.77
14	1972-05-06	5.10	467	−6	−2.86	3.16
15	1972-05-13	5.50	364	−10	−1.04	2.72
16	1972-05-16	18.50	477	−46	−5.43	2.33
17	1972-06-23	6.40	415	−36	−2.81	−1.62
18	1972-06-28	7.20	506	−30	−2.39	−0.74
19	1972-07-04	4.50	349	−4	−0.21	0.27
20	1972-10-11	7.80	396	−36	−2.22	2.21
21	1972-10-19	12.70	429	−52	−0.08	0.54
22	1972-11-01	23.00	520	−133	−13.51	−0.42
23	1972-11-26	5.50	478	−22	−2.56	1.99
24	1972-11-30	5.40	333	−10	−5.45	2.07
25	1972-12-23	9.10	471	−23	−1.28	0.69

Note. "Date" for time of maximal CR decreases, "FD1" represents magnitude of FD from transformed APTY CR data and "ADV1" for magnitude of diurnal anisotropy corresponding to FD1.

Table 2
APTY$_{FD2}$, ADV2 and Solar Wind Data

Order	Date	IMF	SWS	Dst	FD2(%)	ADV2(%)
1	1972-01-02	5.70	438	−11	−0.30	0.18
2	1972-01-30	4.30	490	−20	−1.41	−1.69
3	1972-02-02	6.20	395	−16	−0.76	−1.90
4	1972-02-15	4.40	560	−17	−2.82	−1.83
5	1972-02-20	7.00	447	−28	−3.13	−1.27
6	1972-02-25	4.40	458	−46	−0.67	−0.46
7	1972-03-07	16.00	596	−36	−0.43	1.62
8	1972-03-10	8.60	388	−16	−0.62	2.12
9	1972-04-23	6.50	373	−17	−0.43	2.77
10	1972-05-16	18.50	477	−46	−1.55	2.33
11	1972-06-10	3.70	376	9	−0.29	−2.36
12	1972-06-23	6.40	415	−36	−2.22	−1.62
13	1972-06-28	7.20	506	−30	−1.56	−0.74
14	1972-07-25	12.30	562	−39	−0.66	−1.85
15	1972-10-11	7.80	396	−36	0.00	2.21
16	1972-11-01	23.00	520	−133	−6.96	−0.42
17	1972-11-26	5.50	478	−22	−0.29	1.99
18	1972-11-30	5.40	333	−10	−1.69	2.07
19	1972-12-23	9.10	471	−23	−0.30	0.69

Note. "Date" for time of maximal CR decreases, "FD2" represents magnitude of FD from raw APTY CR data and "ADV2" for magnitude of diurnal anisotropy corresponding to FD2.

The two general approaches to FD identification from CR data include detection of FDs without recourse to solar-wind characteristics (e.g., Pudovkin & Veretenenko 1995; Harrison & Ambaum 2010) and detection of FDs from CR data with solar-wind parameters (e.g., Belov et al. 2009; Ramirez et al. 2013). The association between FD and speculated causative agents like CME, ICME, solar wind speed (SWS), geomagnetic storm index (Dst), IMF, etc. is not yet well understood. In the present work, the link between FD1, FD2, ADV catalogs from APTY and MTWS NM stations and the associated solar-wind data is tested to determine whether the events are real or spurious.

2. Data

The two FD catalogs: FD1 - from Fourier transformed and FD2 - from raw CR data with the corresponding daily ADV based on APTY (Longitude = 43°.28N, Latitude = 42°.69E, $R_c = 5.6$ GV and Altitude = 1700 m) and MTWS (Longitude =44°.27N, Latitude = −71°.30W, $R_c = 1.46$ GV and Altitude =1909 m) high NM detectors are taken from Paper I. IMF, SWS and Dst data are downloaded from omniweb.gsfc.nasa.gov/html/ow data.html.

3. Results and Discussions

3.1. FD1, FD2 and ADV Versus Solar-geophysical Parameters

The magnitudes of FDs and ADV for APTY and MTWS calculated by the FD location algorithm taken from Table 2 in Paper I with the corresponding solar wind parameters are as presented respectively in Tables 1–4. The regression and correlation results of the two FD data sets, ADV and solar wind data for APTY and MTWS detectors are given in Tables 5–8. The statistical significance test of the correlation coefficient (r) is based on the $F_{\text{statistic}}$ indicated on the regression result tables. $F_{\text{statistic}}$ refers to the ratio of two variances that test significance of regression. The plots of the APTY and MTWS FD1 and FD2 versus IMF, SWS, Dst and ADV are displayed, respectively, in Figures 2–5. The corresponding regression Equations (1)–(3) (all not shown) for the graphs reflect the correlation results.

The coefficient of determination (R^2), r and chance probability (p-value) for FD−IMF diagrams in Figures 2(a), 3(a), 4(a) and 5(a) are given in Tables 5–8 respectively. Whereas the FD1−IMF and FD2−IMF respective correlation coefficients of −0.63 and −0.51 at APTY are statistically significant respectively at the 99% and 95% confidence levels, the correlation results for MTWS of −0.32 and −0.14 are statistically non-significant. The regression analysis of the FD −IMF relation at APTY and MTWS may imply that the FD cases from transformed and raw CR data are dependent on IMF intensity.

Table 3
$MTWS_{FD1}$, ADV1 and Solar Wind Data

Order	Date	IMF	SWS	Dst	FD1(%)	ADV1(%)
1	1972-01-02	5.70	438	−11	−0.02	−0.16
2	1972-01-04	4.50	477	−8	−1.52	−0.14
3	1972-01-20	5.20	453	−18	−6.43	0.46
4	1972-01-22	8.90	469	−44	−5.91	0.49
5	1972-02-15	4.40	560	−17	−2.33	−0.08
6	1972-02-19	12.00	441	−34	−5.06	0.02
7	1972-02-25	4.40	458	−46	−1.75	0.46
8	1972-03-03	5.80	402	−22	−0.38	1.33
9	1972-03-07	16.00	596	−36	−3.01	1.92
10	1972-03-12	5.90	466	−7	−3.97	2.66
11	1972-03-29	6.80	472	−17	−1.69	4.11
12	1972-04-05	6.10	620	−17	−2.41	4.21
13	1972-04-07	4.20	443	−15	−2.05	4.22
14	1972-04-23	6.50	373	−17	−3.94	4.31
15	1972-05-03	7.70	466	−14	−0.75	4.07
16	1972-05-06	5.10	467	−6	−1.35	3.83
17	1972-05-13	5.50	364	−10	−0.68	2.84
18	1972-05-16	18.50	477	−46	−7.04	2.23
19	1972-06-23	6.40	415	−36	−3.65	−1.94
20	1972-06-28	7.20	506	−30	−2.72	−0.98
21	1972-10-12	8.10	425	−23	−1.09	0.38
22	1972-11-02	7.20	617	−75	−15.01	−1.35
23	1972-11-26	5.50	478	−22	−3.02	3.15
24	1972-11-29	6.50	381	−24	−3.26	3.22
25	1972-12-02	6.90	278	−1	−1.23	3.14
26	1972-12-06	3.30	272	9	−0.96	2.79
27	1972-12-09	5.40	349	5	−1.29	2.40
28	1972-12-13	9.50	470	−29	−1.67	1.79
29	1972-12-23	9.10	471	−23	−3.78	0.37

Note. "Date" for time of maximal CR decreases, "FD1" represents magnitude of FD from transformed MTWS CR data and "ADV1" for magnitude of diurnal anisotropy associated with FD1.

The FD-SWS plots displayed in Figures 2(b), 3(b), 4(b) and 5(b) yield correlation coefficients of −0.02, −0.26, −0.44 and −0.41 respectively for FD1−SWS and FD2−SWS connections at the two stations.

The FD-Dst relation is very striking. Compared to other parameters, the correlation coefficients for the FD-Dst relation are statistically significant at both stations for all the FD data sets. It is shown to be at the 99% and 95% confidence levels. This suggests that the CR variations at the two stations are driven by geomagnetic storm time activity. Quantitatively, from the R^2 values, Dst index appears to account for more than half of CR depressions in the present data. The plots of FD–ADV relation seem not to show any statistically significant correlations for the two data sets at the two stations

$$FD1_{APTY} = 4.79 \pm 1.10 + (1.11 \pm 0.29)IMF \quad (1)$$

$$FD1_{APTY} = 426.85 \pm 19.49 + (5.21 \pm 0.51)SWS \quad (2)$$

$$FD1_{APTY} = -9.26 \pm 5.76 + (6.57 \pm 1.50)Dst. \quad (3)$$

We have studied the association between two separate FD catalogs (FD1 and FD2), solar-geophysical parameters and the

Table 4
$MTWS_{FD2}$, ADV2 and Solar Wind Data

Order	Date	IMF	SWS	Dst	FD2(%)	ADV2(%)
1	1972-01-02	5.70	438	−11	−0.09	−0.16
2	1972-01-04	4.50	477	−8	−0.83	−0.14
3	1972-01-20	5.20	453	−18	−2.99	0.46
4	1972-01-22	8.90	469	−44	−2.71	0.49
5	1972-02-15	4.40	560	−17	−1.20	−0.08
6	1972-02-19	12.00	441	−34	−2.52	0.02
7	1972-02-25	4.40	458	−46	−0.64	0.46
8	1972-03-07	16.00	596	−36	−0.45	−2.77
9	1972-03-12	5.90	466	−7	−0.66	2.66
10	1972-03-16	10.10	374	−34	−2.41	2.23
11	1972-05-16	18.50	477	−46	−2.41	2.22
12	1972-06-11	4.00	336	15	−0.29	−3.05
13	1972-06-23	6.40	415	−36	−2.79	−1.94
14	1972-06-28	7.20	506	−30	−1.85	−0.98
15	1972-07-26	5.70	543	−26	−0.90	−3.60
16	1972-10-12	8.10	425	−23	−0.36	0.38
17	1972-10-20	8.50	483	−32	−0.16	−1.39
18	1972-10-23	5.70	409	−36	−0.36	−1.75
19	1972-11-02	7.20	617	−75	−8.18	−1.35
20	1972-11-29	6.50	381	−24	−0.02	3.23
21	1972-12-23	9.10	471	−23	−1.71	0.37

Note. "Date" for time of maximal CR decreases, "FD2" represents magnitude of FD from raw MTWS CR data and "ADV2" for magnitude of diurnal anisotropy associated with FD2.

Table 5
APTY FD1 Regression Results with other Parameters; $F_{critical} = 7.88$ (99% Confidence)

Order	Parameter	R^2	r	p-value	$F_{statistic}$
1	FD1–IMF	0.40	−0.63	7.62×10^{-04}	15.04
2	FD1–SWS	0.04	−0.02*	0.32	1.05
3	FD1–Dst	0.45	0.67	2.24×10^{-04}	19.09
4	FD1–ADV	0.02	0.14*	0.49	0.48

Note. Non-statistically significant correlations are marked with *. "Order" stands for the sequence of parameters, R^2 denotes coefficient of determination, r represents coefficient of correlation, p-value is the chance probability and $F_{statistic}$ refers to ratio of two variances that test significance of regression.

Table 6
APTY FD2 Regression Results with other Variables; $F_{critical} = 4.45$; (95% Confidence)

Order	Variable	R^2	r	p-value	$F_{statistic}$
1	FD2–IMF	0.26	−0.51	0.02	6.08
2	FD2–SWS	0.07	−0.26*	0.29	1.20
3	FD2–Dst	0.58	0.76	1.53×10^{-04}	23.45
4	FD2–ADV	0.07	0.27*	0.26	1.36

Note. Non-statistically significant correlations are marked with *. Parameters are as defined in Table 5.

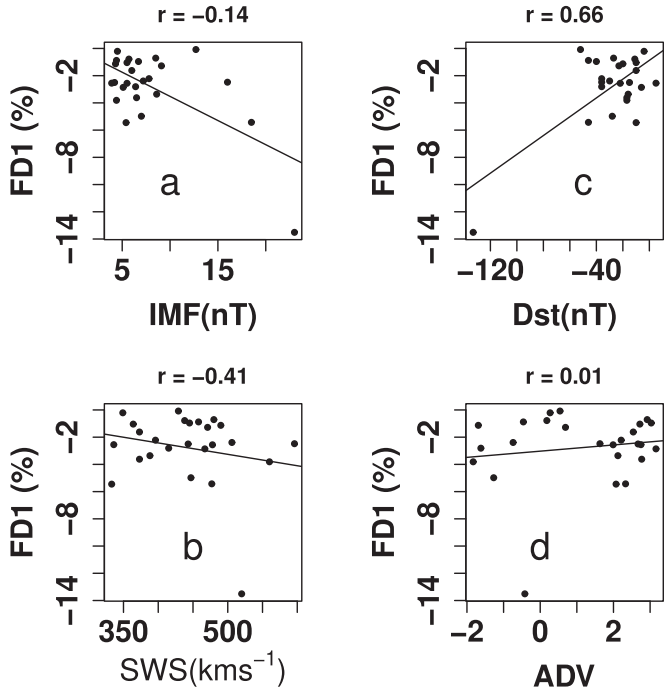

Figure 2. Scatter Plots of Magnitude of $FD1_{APTY}$ versus Solar Wind Parameters and CR Diurnal Anisotropy.

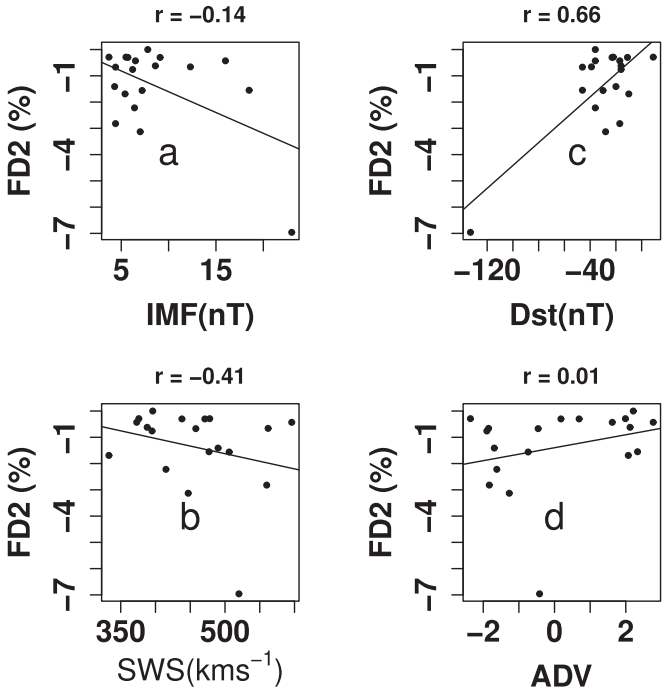

Figure 3. Graph of Amplitude of $FD2_{APTY}$ versus Solar Wind Parameters and CR Diurnal Anisotropy.

Table 7
MTWS FD1 Regression Results with other Variables; $F_{critical} = 4.21$; (95% Confidence)

Order	Variable	R^2	r	p-value	$F_{statistic}$
1	FD1–IMF	0.10	−0.32	0.09*	3.03
2	FD1–SWS	0.19	−0.44	0.02	6.44
3	FD1–Dst	0.55	0.74	4.75×10^{-06}	32.42
4	FD1–ADV	0.13	0.36	0.06*	3.99

Note. Non-statistically significant correlations are marked with *. Parameters are as defined in Table 5.

Table 8
MTWS FD2 Regression Results with other Variables; $F_{critical} = 4.38$; (95% Confidence)

Order	Variable	R^2	r	p-value	$F_{statistic}$
1	FD2–IMF	0.02	−0.14*	0.55	0.36
2	FD2–SWS	0.17	−0.41*	0.07	3.81
3	FD2–Dst	0.44	0.66	0.001	14.98
4	FD2–ADV	0.0002	0.01*	0.96	0.003

Note. Non-statistically significant correlations are marked with *. Parameters are as defined in Table 5.

associated magnitudes of diurnal anisotropies observed at APTY and MTWS stations during the year 1972 which is a period of high solar activity. The results of FD1−IMF, FD1−Dst at APTY; FD1−SWS, FD1−Dst at MTWS which are statistically significant are consistent with the submission of Okike (2019) that found statistically significant correlations for FD–IMF ($r = -0.39$), FD−SWS ($r = -0.71$) and FD−Dst ($r = 0.45$) for the processed CR data. FD1−SWS at APTY and FD1−IMF at MTWS that are statistically non-significant do not reflect their findings.

Using a total of 17 and 68 FD events respectively, Kane (2010) and Lingri et al. (2016) investigated the connection between FD amplitude and Dst index but did not find any discernible pattern between the two parameters. Belov et al. (2001) found a correlation coefficient $r < 0.42$ between FD and Dst. We find statistically significant FD2−Dst correlations contrary to their reports. This could be an indication of the differences in the semi-automated and the present fully automated FD event identification approaches (Alhassan et al. 2021). Okike (2020b), from a critique of the traditional manual technique of determination of the magnitude of FDs, reported correlation coefficients for FD−Dst and FD−SWS relations at three CR stations: ESOI station (ESOI), McMurdo (MCMD) and Thule (THUL) respectively as 0.18, 0.34, 0.32 and 0.00, −0.11, −0.12. The non-statistically significant results we obtained here for FD2−SWS of $r = -0.26$ for APTY and −0.41 for MTWS are at variance with their result. Our result suggests that different mechanisms might be responsible for the FDs and SWS. The FD2−Dst results of $r = 0.76$ and $r = 0.66$ respectively for APTY and MTWS NMs reported in the current analysis agree with their finding.

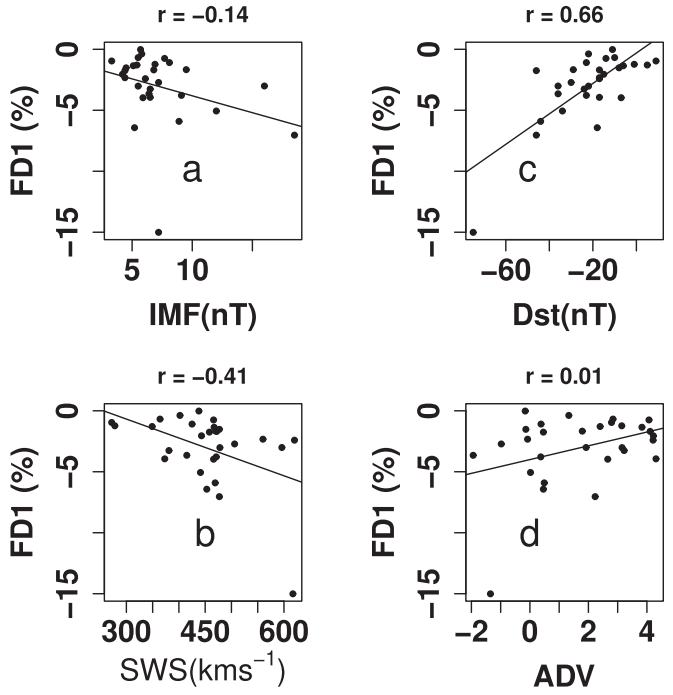

Figure 4. Plots of $FD1_{MTWS}$ Magnitude, Solar Wind Parameters and Magnitude of CR Diurnal wave.

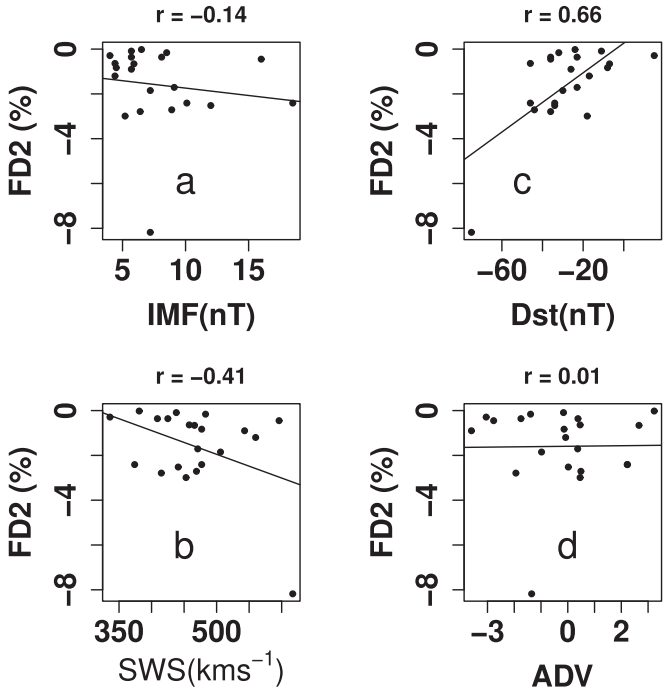

Figure 5. Correlation between $FD2_{MTWS}$ Event sizes, Solar Wind Parameters and Magnitude of CR Diurnal Wave.

In an important review of FDs, Lockwood (1971) suggested that IMF and Dst are responsible for the high-frequency modulation of CRs. The strong connection between the amplitude of FD and Dst activity for the two data sets at the 99% and 95% confidence levels and FD−IMF relation at APTY for the two FD catalogs, significant at the 99% and 95% confidence levels reported here, is consistent with their proposition. In the context of previous publications, we report that these two types of magnetic fields (the interplanetary (IMF) and geomagnetic (Dst)) could be the causative agents of the high frequency variation of CRs. Recently, Alhassan et al. (2021) found statistically significant correlations between FDs from raw CR data, IMF, SWS and Dst. The current results for FD2−IMF, FD2−Dst for APTY and FD2−Dst for MTWS reflect the finding of these authors. Our results of FD2−SWS at APTY and FD2−IMF, FD2−SWS at MTWS are contrary to their submissions. These present findings show that the mechanisms responsible for FD, IMF and SWS are not the same and also that IMF and SWS may not play significant roles in CR modulations when unprocessed data are considered as previously reported. This may also be due to the masking effect of diurnal anisotropy on the CR data.

CR anisotropy has been identified as an important signal in CR flux intensity reductions by Okike (2021). For this reason, a linear relationship between the amplitude of FDs and the magnitude of the CR diurnal wave should be envisaged. We examined this relationship and found that there exists no statistically significant correlation between FD1, FD2 and the amplitude of the diurnal oscillation. Our regression analysis does not reflect the results of Okike (2021) in which significant correlation was reported especially between FD1 and ADV. This trend is understandable in light of the findings of Paper I. Paper I demonstrated that it is difficult to determine a pattern between FDs and ADV. This is due to the fact that in some cases, anisotropy tends to reduce the magnitude of FDs or enhance it. In some other cases, the effect seems negligible. The association between them is quite complex and does not seem to have a definite pattern.

3.2. GCR Modulation Dependence on Rigidity/NM Efficiency

It has been reported that an asymptotic cone of acceptance and geomagnetic cutoff rigidity determines whether a given NM observes an increasing or decreasing GCR flux (Smart & Shea 2003; D'Andrea et al. 2009). This has been attributed to the fact that the distribution of GCR flux over the Earth is asymmetrical, but could be the result of the association between the IMF and the geomagnetic field at a particular location on Earth. We test the proposition that the monitors with the lowest vertical cutoff rigidity could be more sensitive to variation in counting rate with FDs observed at APTY and MTWS with different rigidities taken from Table 2 in Paper I. For the largest event on 1972 August 5, the magnitudes at

APTY and MTWS are −25.49% and −29.22% respectively. From the event on 1972 June 18, −7.50% and −8.57% magnitudes were calculated for APTY and MTWS respectively. For the smallest event on 1972 January 2, the amplitude at APTY is −0.78% while that at MTWS is −0.02%. Examining the corresponding events at the two stations, we observe that, on average, the NM at MTWS that is characterized by low vertical cutoff rigidity is more sensitive to CR intensity variations during FDs than the detector at APTY with higher rigidity. This result is consistent with the findings of Okike (2020b).

4. Conclusions

Raw CR data are characterized by high variability and different superposed signals of dissimilar periodicities, cycles and recurrences such as FDs, diurnal anisotropies, SEPs and GLEs (Okike 2021). The measurement of the magnitude of FDs and the accurate timing of its occurrence will be difficult to achieve with the manual FD detection method. Application of Fourier transform to isolated NM data is capable of filtering out undesirable signals superposed on raw CR counts. This led to the identification of two FD catalogs and ADV from filtered (FD1 and ADV) and raw (FD2) CR data by Paper I. Establishing the link between FD and solar-geophysical activity indices as a means of validating the FD list is still poorly understood as existing publications yield conflicting results. The conflicting submissions may be argued to stem from different FD data identified by investigators using different NM data.

The two-dimensional regression analysis carried out in this study reveals that two types of magnetic fields - interplanetary (IMF) and geomagnetic (Dst) - appear to be responsible for FD detection as evident from FD−IMF/Dst statistically significant correlations. We did not find evidence of significant FD−ADV correlation from the two FD catalogs. This could be due to the complex link between FD and ADV.

Acknowledgments

We feel indebted to the group maintaining the website omniweb.gsfc.nasa.gov/html/owdata.html from where we downloaded the solar-geophysical data. The members of the R-mailing list (R-help@r-project.org) are gratefully acknowledged for assistance in codes for the preliminary data analysis stage of the work. The invaluable contributions of the anonymous referee are hereby appreciated.

Appendix
Abbreviations and Definitions

We have used many abbreviations in the text. To assist the reader, a list of abbreviations and definitions is provided in Table 9.

Table 9
Abbreviations and Definitions

S/N	Abbreviation	Definition
1	CR	Cosmic ray
2	FD	Forbush decrease
3	ADV	Amplitude diurnal variation
4	FD1	Forbush decrease from filtered cosmic ray data
5	FD2	Forbush decrease from raw cosmic ray data
6	IMF	Interplanetary magnetic field
7	Dst	Geomagnetic storm index
8	GCR	Galactic cosmic ray
9	NMs	Neutron monitors
10	IPDs	Interplanetary disturbances
11	CMEs	Coronal mass ejections
12	ICMEs	Interplanetary coronal mass ejections
13	CHs	Coronal holes
14	SEPs	Solar energetic particles
15	GLEs	Ground level enhancements
16	FFT	Fast Fourier transformation
17	CLMX	Climax
18	APTY	Apatity
19	MTWS	Mt. Washington
20	SWS	Solar wind speed
21	MCMD	McMurdo
22	THUL	Thule

References

Alhassan, J. A., Okike, O., & Chukwude, A. E. 2021, RAA, 21, 1
Axford, W. I. 1965, P&SS, 12, 115
Barouch, E., & Burlaga, L. F. 1975, JGR, 80, 449
Belov, A., Abunin, A., Abunina, M., et al. 2014, SoPh, 289, 3949
Belov, A. V., Asipenka, A., Dryn, E. A., et al. 2009, BRASP, 73, 331
Belov, A. V., Eroshenko, E. A., Oleneva, V. A., Struminsky, A. B., & Yanke, V. G. 2001, AdSpR, 27, 625
Belov, A. V. 2008, in Universal Heliophysical Processes, Proc. IAU Symp., 257
Cane, H. V., & Richardson, I. G. 2003, JGR, 108, 1
Cane, H. V., Richardson, I. G., & von Rosenvinge, T. T. 1996, JGR, 101, 21561
D'Andrea, C., Poirier, J., & Balsara, D. S. 2009, AdSpR, 44, 1247
Forbush, S. E. 1938, PhRv, 54, 975
Harrison, R., & Ambaum, M. 2010, JASTP, 72, 1408
Kane, R. P. 2010, AnGeo, 28, 479
Lingri, D., Mavromichalaki, H., Belov, A., et al. 2016, SoPh, 291, 1025
Lockwood, J. A. 1971, SSRv, 12, 658
McCracken, K. G., & Rau, U. R. 1965, in Proc. ICRC, 213M *(Dallas, TX)*, 1
Melkumyan, A. A., Belov, A. V., Abunina, M. A., et al. 2019, STP, 5, 28
Oh, S., Yi, Y., & Kim, H. Y. 2008, JGR, 113, A01103
Okike, O. 2019, JGRA, 124, 1
Okike, O. 2020a, JASTP, 211, 1364
Okike, O. 2020b, MNRAS, 491, 3793
Okike, O. 2021, ApJ, 60, 915
Okike, O., & Alhassan, J. A. 2021, SoPh, 296, 112
Okike, O., Alhassan, J. A., Iyida, E. U., & Chukwude, A. E. 2021, MNRAS, 503, 5676
Okike, O., & Umahi, A. E. 2019, SoPh, 294, 16
Pudovkin, M. I., & Veretenenko, S. V. 1995, JASTP, 57, 1349
Ramirez, O. O. U., Galicia, J. F. V., Munoz, G., & Huttunen, E. 2013, in 33rd Proc. ICRC *(Rio de Janeiro)*, 1967
Rao, U. 1976, SSRv, 19, 533
Richardson, I. G., & Cane, H. V. 2011, SoPh, 8, 609
Smart, D. F., & Shea, M. A. 2003, AdSpR, 32, 109